Original Article

Journal of Intelligent Material Systems and Structures

Journal of Intelligent Material Systems and Structures
2017, Vol. 28(19) 2688–2704
© The Author(s) 2017
Reprints and permissions:
sagepub.co.uk/journalsPermissions.nav
DOI: 10.1177/1045389X17698241
journals.sagepub.com/home/jim
SAGE

Benchmark solutions for the free vibration of layered piezoelectric plates based on a variational formulation

Gennady M Kulikov and Svetlana V Plotnikova

Abstract

This article focuses on the implementation of the sampling surfaces method for the three-dimensional vibration analysis of layered piezoelectric plates. The sampling surfaces method is based on choosing inside the layers not equally spaced sampling surfaces parallel to the middle surface in order to introduce the displacements and electric potentials of these surfaces as basic plate variables. Such choice of unknowns with the consequent use of Lagrange polynomials in the assumed distributions of displacements, strains, electric potential, and electric field vector through the thicknesses of layers leads to the robust piezoelectric plate formulation. The sampling surfaces are located inside each layer at Chebyshev polynomial nodes that makes it possible to minimize uniformly the error due to the Lagrange interpolation. Therefore, the sampling surfaces formulation can be applied efficiently to the obtaining of benchmark solutions for the free vibration of layered piezoelectric plates, which asymptotically approach the three-dimensional solutions of piezoelectricity as the number of sampling surfaces tends to infinity.

Keywords

Three-dimensional vibration, piezoelectric plate, Ritz solution, sampling surfaces formulation

Introduction

Three-dimensional (3D) vibration analysis of layered piezoelectric plates has received considerable attention during past 20 years. There are at least four approaches to 3D exact solutions of electroelasticity for layered piezoelectric plates, namely, the Pagano approach (Pagano, 1970), the state space approach (Brogan, 1985), the power series expansion approach, that is, the Frobenius method (Frobenius, 1873), and the asymptotic expansion approach, that is, the perturbation method (Gol'denveizer, 1961). These approaches are discussed in survey articles (Wu et al., 2008; Wu and Liu, 2016). The Pagano approach was implemented for the freely vibrating simply supported piezoelectric plates (Heyliger and Brooks, 1995; Heyliger and Saravanos, 1995) and extended then to the transient response of piezoelectric and magnetostrictive plates subjected to nonuniform heating (Ootao and Tanigawa, 2000, 2005). The most popular state space approach was extensively utilized for solving the dynamic problems of simply supported electroelastic plates by Chen et al. (1998), Ding et al. (1999), Chen and Ding (2002), Deü and Benjeddou (2005), and Zhong and Yu (2006) and magneto-electroelastic plates by Pan and Heyliger (2002), Chen et al. (2005), and Chen et al. (2007a, 2007b). Messina and Carrera (2015) proposed to utilize the transfer matrix method to solve the ordinary differential equations in terms of the displacements and electric potential derived from the system of partial differential equations through the separating variable procedure. The dynamic response of laminated piezoelectric plates through Taylor series expansions in the thickness direction was studied by Gao et al. (1998), Vel et al. (2004), and Baillargeon and Vel (2005). The asymptotic approach was also implemented effectively for stress and vibration analyses of piezoelectric and magnetostrictive plates and shells (Cheng and Batra, 2000; Cheng et al., 2000; Kalamkarov and Kolpakov, 2001; Reddy and Cheng, 2001; Tsai and Wu, 2008; Vetyukov et al., 2011). However, the discussed approaches are not easy to implement for the 3D dynamic analysis of layered piezoelectric plates with general boundary conditions.

Laboratory of Intelligent Materials and Structures, Tambov State Technical University, Tambov, Russia

Corresponding author:
Gennady M Kulikov, Laboratory of Intelligent Materials and Structures, Tambov State Technical University, 106, Sovetskaya Street, Tambov 392000, Russia.
Email: gmkulikov@mail.ru

In the literature, there is a powerful tool to overcome the above-mentioned difficulties. This is a sampling surfaces (SaS) method developed recently by the authors and the SaS-based variational formulation. The SaS method was utilized first for the 3D stress and vibration analyses of elastic composite plates and shells (Kulikov and Plotnikova, 2011; Kulikov et al., 2016). According to this method, one chooses the arbitrarily located surfaces inside the nth layer $\Omega^{(n)1}$, $\Omega^{(n)2}$, …, $\Omega^{(n)I_n}$ parallel to the middle surface in order to introduce the displacement vectors $\mathbf{u}^{(n)1}$, $\mathbf{u}^{(n)2}$,…, $\mathbf{u}^{(n)I_n}$ and electric potentials $\varphi^{(n)1}$, $\varphi^{(n)2}$,…, $\varphi^{(n)I_n}$ of these surfaces as basic plate unknowns, where I_n is the number of SaS of the nth layer ($I_n \geq 3$). Such choice of unknowns with the consequent use of the Lagrange polynomials of degree $I_n - 1$ in assumed through-thickness distributions of the displacements, strains, electric potential, and electric field vector of the nth layer leads to a robust piezoelectric plate formulation. Note that the SaS formulation has been implemented only for the 3D stress analysis of layered and functionally graded piezoelectric plates and shells (Kulikov et al., 2015; Kulikov and Plotnikova, 2013a, 2013b, 2013c, 2014, 2015, 2017). This article is intended to extend the SaS formulation to the vibration analysis of piezoelectric plates and present the benchmark solutions for the free vibration of layered piezoelectric plates.

It should be noted that the SaS plate formulation with equally spaced SaS does not work properly with the Lagrange polynomials of high degree because of Runge's phenomenon. This phenomenon yields the wild oscillation at the edges of the interval when the user deals with some specific functions (Burden and Faires, 2010). If the number of equispaced nodes increased, then the oscillations become even larger. However, the use of the Chebyshev polynomial nodes inside the plate body (Kulikov et al., 2016; Kulikov and Plotnikova, 2013a, 2013c, 2015) can help to improve significantly the behavior of the Lagrange polynomials of high degree because such a choice makes it possible to minimize uniformly the error due to the Lagrange interpolation. This fact gives an opportunity to obtain the displacements and stresses with a prescribed accuracy employing the sufficiently large number of SaS. It means in turn, the solutions based on the SaS concept asymptotically approach the 3D exact solutions of elasticity as the number of SaS $I_n \to \infty$.

The origins of the SaS concept can be found in contributions (Kulikov, 2001; Kulikov and Carrera, 2008) in which three, four, and five equally spaced SaS are employed. The SaS formulation with the arbitrary number of equispaced SaS is considered by Kulikov and Plotnikova (2011). The more general approach with the SaS located at Chebyshev polynomial nodes was developed later (Kulikov et al., 2015; Kulikov and Plotnikova, 2013b, 2014). Also note that the term SaS should not be confused with such terms as mathematical or virtual surfaces extensively utilized in Carrera's unified formulation (CUF; Carrera, 2002, 2003), which was implemented for the 3D vibration analysis of laminated piezoelectric plates and shells (Carrera et al., 2010, 2011; D'Ottavio et al., 2006). This is due to the fact that in a CUF, the generalized displacements of layers having no mechanical sense are used. On the contrary, in a SaS plate formulation, all basic variables including the strains and electric field components are related to SaS of layers.

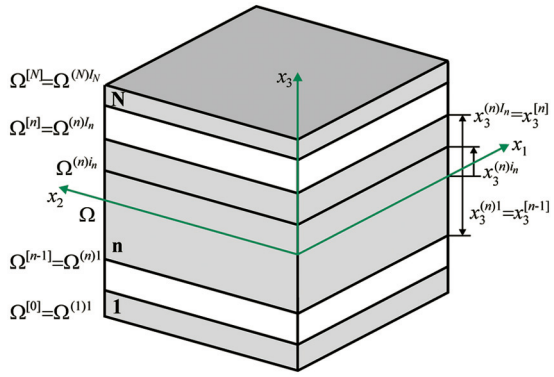

Figure 1. Geometry of the laminated plate.

Kinematic description of layered plate

Consider a layered plate of thickness h. Let the middle surface Ω be described by Cartesian coordinates x_1 and x_2. The coordinate x_3 is oriented in the thickness direction. According to the SaS concept, we choose inside each layer I_n SaS $\Omega^{(n)1}$, $\Omega^{(n)2}$,…, $\Omega^{(n)I_n}$ parallel to the middle surface. The transverse coordinates of SaS of the nth layer are given by

$$x_3^{(n)1} = x_3^{[n-1]}, \quad x_3^{(n)I_n} = x_3^{[n]} \tag{1}$$

$$x_3^{(n)m_n} = \frac{1}{2}\left(x_3^{[n-1]} + x_3^{[n]}\right) - \frac{1}{2}h_n \cos\left(\pi \frac{2m_n - 3}{2(I_n - 2)}\right) \tag{2}$$

where $x_3^{[n-1]}$ and $x_3^{[n]}$ are the transverse coordinates of interfaces $\Omega^{[n-1]}$ and $\Omega^{[n]}$ depicted in Figure 1; $h_n = x_3^{[n]} - x_3^{[n-1]}$ is the thickness of the nth layer; the index n identifies the belonging of any quantity to the nth layer and runs from 1 to N, where N is the number of layers; the index m_n identifies the belonging of any quantity to inner SaS of the nth layer and runs from 2 to $I_n - 1$; the indices i_n, j_n, and k_n to be introduced later for describing all SaS of the nth layer running from 1 to I_n.

It is important that the transverse coordinates of inner SaS (2) coincide with the coordinates of Chebyshev polynomial nodes (Burden and Faires, 2010). This fact has a great meaning for a convergence of the SaS method (Kulikov and Plotnikova, 2013b, 2014).

The strains of the nth layer $\varepsilon_{ij}^{(n)}$ are given by

$$2\varepsilon_{\alpha\beta}^{(n)} = u_{\alpha,\beta}^{(n)} + u_{\beta,\alpha}^{(n)}$$
$$2\varepsilon_{\alpha 3}^{(n)} = \beta_{\alpha}^{(n)} + u_{3,\alpha}^{(n)}, \quad \varepsilon_{33}^{(n)} = \beta_{3}^{(n)} \tag{3}$$

where $u_i^{(n)}$ are the displacements of the nth layer; $\beta_i^{(n)}$ are the derivatives of displacements with respect to the thickness coordinate

$$\beta_i^{(n)} = u_{i,3}^{(n)} \tag{4}$$

Here and throughout this article, Latin indices i, j, k, l range from 1 to 3, whereas Greek indices α, β range from 1 to 2; the symbol $(\ldots)_{,i}$ stands for the partial derivatives with respect to coordinate x_i.

Introduce displacements of SaS of the nth layer $u_i^{(n)i_n}(x_1, x_2)$ as basic plate unknowns as follows

$$u_i^{(n)i_n} = u_i^{(n)}(x_3^{(n)i_n}) \tag{5}$$

Due to boundary conditions at outer surfaces and continuity conditions at interfaces, we have

$$u_i^{(1)1} = u_i^{[0]}, \quad u_i^{(N)I_N} = u_i^{[N]} \tag{6}$$

$$u_i^{(m)I_m} = u_i^{(m+1)1} = u_i^{[m]} \tag{7}$$

where $u_i^{[0]}(x_1, x_2)$ and $u_i^{[N]}(x_1, x_2)$ are the displacements of bottom and top surfaces; $u_i^{[m]}(x_1, x_2)$ are the displacements of interfaces; the index m stands for the number of interfaces and runs from 1 to $N-1$.

Next, we introduce strains of SaS of the nth layer $\varepsilon_{ij}^{(n)i_n}(x_1, x_2)$ as

$$\varepsilon_{ij}^{(n)i_n} = \varepsilon_{ij}^{(n)}(x_3^{(n)i_n}) \tag{8}$$

Using equations (3) to (5) and (8) leads to relations between the SaS variables

$$2\varepsilon_{\alpha\beta}^{(n)i_n} = u_{\alpha,\beta}^{(n)i_n} + u_{\beta,\alpha}^{(n)i_n}$$
$$2\varepsilon_{\alpha 3}^{(n)i_n} = \beta_{\alpha}^{(n)i_n} + u_{3,\alpha}^{(n)i_n}, \quad \varepsilon_{33}^{(n)i_n} = \beta_{3}^{(n)i_n} \tag{9}$$

where $\beta_i^{(n)i_n}(x_1, x_2)$ are the values of derivatives of displacements with respect to the thickness coordinate at SaS of the nth layer

$$\beta_i^{(n)i_n} = \beta_i^{(n)}(x_3^{(n)i_n}) \tag{10}$$

Up to this moment, no assumptions concerning the displacement field have been made. We start now with the first assumption of the proposed higher-order layer-wise plate formulation. Let us assume that the displacements are distributed through the thickness in the following form

$$u_i^{(n)} = \sum_{i_n} L^{(n)i_n} u_i^{(n)i_n}, \quad x_3^{[n-1]} \le x_3 \le x_3^{[n]} \tag{11}$$

where $L^{(n)i_n}(x_3)$ are the Lagrange polynomials of degree $I_n - 1$ defined as

$$L^{(n)i_n} = \prod_{j_n \ne i_n} \frac{x_3 - x_3^{(n)j_n}}{x_3^{(n)i_n} - x_3^{(n)j_n}} \tag{12}$$

Substituting SaS approximation (11) in (4) results in

$$\beta_i^{(n)} = \sum_{i_n} M^{(n)i_n} u_i^{(n)i_n} \tag{13}$$

where $M^{(n)i_n} = L_{,3}^{(n)i_n}$ are the polynomials of degree $I_n - 2$.

Taking into consideration the identity

$$M^{(n)i_n} = \sum_{j_n} M^{(n)i_n}(x_3^{(n)j_n}) L^{(n)j_n} \tag{14}$$

which follows directly from the fundamental property of the Lagrange polynomials $L^{(n)j_n}$, one obtains

$$\beta_i^{(n)} = \sum_{i_n} L^{(n)i_n} \beta_i^{(n)i_n} \tag{15}$$

where

$$\beta_i^{(n)i_n} = \sum_{j_n} M^{(n)j_n}(x_3^{(n)i_n}) u_i^{(n)j_n} \tag{16}$$

The derivatives of the Lagrange polynomials at SaS $M^{(n)j_n}(x_3^{(n)i_n})$ are evaluated in accordance with (Kulikov et al., 2016; Kulikov and Plotnikova, 2013a).

It is seen from equation (16) that the key functions $\beta_i^{(n)i_n}$ of the SaS layered plate formulation are represented as a *linear combination* of displacements of SaS of the nth layer $u_i^{(n)j_n}$.

Proposition 1. The functions $\beta_i^{(n)1}, \beta_i^{(n)2}, \ldots, \beta_i^{(n)I_n}$ are linearly dependent, that is, there exist numbers $\alpha^{(n)1}, \alpha^{(n)2}, \ldots, \alpha^{(n)I_n}$, which are not all zero such that

$$\sum_{i_n} \alpha^{(n)i_n} \beta_i^{(n)i_n} = 0 \tag{17}$$

The proof of this statement can be found in Kulikov and Plotnikova (2016).

Substituting the displacement approximations (11) and (15) into strain-displacement relations (3) and using (9), we arrive at the distribution of strains through the thickness of the nth layer

$$\varepsilon_{ij}^{(n)} = \sum_{i_n} L^{(n)i_n} \varepsilon_{ij}^{(n)i_n}, \quad x_3^{[n-1]} \le x_3 \le x_3^{[n]} \tag{18}$$

As can be seen, the through-thickness strain distribution (18) is similar to the displacement distribution (11). This is important because the strains of the nth layer explicitly depend on the SaS strains of the same layer.

Description of electric field

The relation between the electric field $E_i^{(n)}$ and the electric potential $\varphi^{(n)}$ of the nth layer is given by

$$E_\alpha^{(n)} = -\varphi_{,\alpha}^{(n)}, \quad E_3^{(n)} = -\psi^{(n)} \tag{19}$$

where

$$\psi^{(n)} = \varphi_{,3}^{(n)} \tag{20}$$

Introduce electric potentials of SaS of the nth layer $\varphi^{(n)i_n}(x_1, x_2)$ as a second set of basic plate unknowns by

$$\varphi^{(n)i_n} = \varphi^{(n)}(x_3^{(n)i_n}) \tag{21}$$

Due to boundary conditions at outer surfaces and continuity conditions at interfaces, we have

$$\varphi^{(1)1} = \varphi^{[0]}, \quad \varphi^{(N)I_N} = \varphi^{[N]} \tag{22}$$

$$\varphi^{(m)I_m} = \varphi^{(m+1)1} = \varphi^{[m]} \tag{23}$$

where $\varphi^{[0]}(x_1, x_2)$ and $\varphi^{[N]}(x_1, x_2)$ are the electric potentials of bottom and top surfaces; $\varphi^{[m]}(x_1, x_2)$ are the electric potentials of interfaces.

Introduce then the electric field components at SaS of the nth layer $E_i^{(n)i_n}$ as

$$E_i^{(n)i_n} = E_i^{(n)}(x_3^{(n)i_n}) \tag{24}$$

Using equations (19) to (21) and (24) leads to relations between the SaS variables

$$E_\alpha^{(n)i_n} = -\varphi_{,\alpha}^{(n)i_n}, \quad E_3^{(n)i_n} = -\psi^{(n)i_n} \tag{25}$$

where $\psi^{(n)i_n}(x_1, x_2)$ are the values of the derivative of the electric potential of the nth layer with respect to coordinate x_3 at SaS

$$\psi^{(n)i_n} = \psi^{(n)}(x_3^{(n)i_n}) \tag{26}$$

Now, we accept the second assumption of the SaS layered piezoelectric plate formulation. Assume that the electric potential is distributed through the thickness of the nth layer according to the SaS concept as

$$\varphi^{(n)} = \sum_{i_n} L^{(n)i_n}\varphi^{(n)i_n}, \quad x_3^{[n-1]} \le x_3 \le x_3^{[n]} \tag{27}$$

Substituting SaS approximation (27) in (20) yields

$$\psi^{(n)} = \sum_{i_n} M^{(n)i_n}\varphi^{(n)i_n} \tag{28}$$

Using again the identity (14), one obtains

$$\psi^{(n)} = \sum_{i_n} L^{(n)i_n}\psi^{(n)i_n} \tag{29}$$

where

$$\psi^{(n)i_n} = \sum_{j_n} M^{(n)j_n}(x_3^{(n)i_n})\varphi^{(n)j_n} \tag{30}$$

that is similar to equation (16). This means that the key functions $\psi^{(n)i_n}$ of the SaS layered piezoelectric plate formulation are represented as a *linear combination* of electric potentials of SaS of the nth layer $\varphi^{(n)j_n}$.

Proposition 2. The functions $\psi^{(n)1}, \psi^{(n)2}, \ldots, \psi^{(n)I_n}$ are linearly dependent, that is, there exist numbers $\gamma^{(n)1}, \gamma^{(n)2}, \ldots, \gamma^{(n)I_n}$, which are not all zero such that

$$\sum_{i_n} \gamma^{(n)i_n}\psi^{(n)i_n} = 0 \tag{31}$$

This statement could be proved by using the technique developed by Kulikov and Plotnikova (2016).

Substituting the through-thickness approximations (27) and (29) in relations (19) and using (25), we arrive at the distribution of the electric field through the thickness of the nth layer

$$E_i^{(n)} = \sum_{i_n} L^{(n)i_n}E_i^{(n)i_n}, \quad x_3^{[n-1]} \le x_3 \le x_3^{[n]} \tag{32}$$

Variational formulation of piezoelectric plate problem

In the case of free vibrations of the layered piezoelectric plate when no external loads are applied, the extended Hamilton's principle (Tiersten, 1969) is written as

$$\delta \int_{t_1}^{t_2} (T - \Pi)dt = 0 \tag{33}$$

where t_1 and t_2 are two specified times; T is the kinetic energy; Π is the electromechanical energy given by

$$T = \frac{1}{2}\iint_\Omega \sum_n \int_{x_3^{[n-1]}}^{x_3^{[n]}} \rho^{(n)}\dot{u}_i^{(n)}\dot{u}_i^{(n)}dx_1dx_2dx_3 \tag{34}$$

$$\Pi = \frac{1}{2}\iint_\Omega \sum_n \int_{x_3^{[n-1]}}^{x_3^{[n]}} (\sigma_{ij}^{(n)}\varepsilon_{ij}^{(n)} - D_i^{(n)}E_i^{(n)})dx_1dx_2dx_3 \tag{35}$$

where $\sigma_{ij}^{(n)}$ are the components of the stress tensor of the nth layer; $D_i^{(n)}$ are the components of the electric displacement vector of the nth layer; $\rho^{(n)}$ is the mass density of the nth layer; $\dot{u}_i^{(n)}$ is the derivative of displacements with respect to time t. Here and in the following developments, the summation on repeated Latin indices is implied.

Substituting strain and electric field distributions (18) and (32) in (35) and introducing stress resultants

$$H_{ij}^{(n)i_n} = \int_{x_3^{[n-1]}}^{x_3^{[n]}} \sigma_{ij}^{(n)} L^{(n)i_n} dx_3 \tag{36}$$

and electric displacement resultants

$$T_i^{(n)i_n} = \int_{x_3^{[n-1]}}^{x_3^{[n]}} D_i^{(n)} L^{(n)i_n} dx_3 \tag{37}$$

one obtains

$$\Pi = \frac{1}{2}\iint_{\Omega} \sum_n \sum_{i_n} \left(H_{ij}^{(n)i_n} \varepsilon_{ij}^{(n)i_n} - T_i^{(n)i_n} E_i^{(n)i_n} \right) dx_1 dx_2 \tag{38}$$

For simplicity, we consider the case of linear piezoelectric materials. Therefore, the constitutive equations are written as follows

$$\sigma_{ij}^{(n)} = C_{ijkl}^{(n)} \varepsilon_{kl}^{(n)} - e_{kij}^{(n)} E_k^{(n)}, \quad x_3^{[n-1]} \le x_3 \le x_3^{[n]} \tag{39}$$

$$D_i^{(n)} = e_{ikl}^{(n)} \varepsilon_{kl}^{(n)} + \in_{ik}^{(n)} E_k^{(n)}, \quad x_3^{[n-1]} \le x_3 \le x_3^{[n]} \tag{40}$$

where $C_{ijkl}^{(n)}$, $e_{kij}^{(n)}$, and $\in_{ijk}^{(n)}$ are the elastic, piezoelectric, and dielectric constants of the nth layer.

Inserting constitutive equations (39) and (40) correspondingly in (36) and (37) and using again through-thickness distributions (18) and (32), we have

$$H_{ij}^{(n)i_n} = \sum_{j_n} \Lambda^{(n)i_n j_n} \left(C_{ijkl}^{(n)} \varepsilon_{kl}^{(n)j_n} - e_{kij}^{(n)} E_k^{(n)j_n} \right) \tag{41}$$

$$T_i^{(n)i_n} = \sum_{j_n} \Lambda^{(n)i_n j_n} \left(e_{ikl}^{(n)} \varepsilon_{kl}^{(n)j_n} + \in_{ik}^{(n)} E_k^{(n)j_n} \right) \tag{42}$$

where $\Lambda^{(n)i_n j_n}$ are the weighted coefficients defined as

$$\Lambda^{(n)i_n j_n} = \int_{x_3^{[n-1]}}^{x_3^{[n]}} L^{(n)i_n} L^{(n)j_n} dx_3 \tag{43}$$

Substituting equations (11) and (41), (42) correspondingly in (34) and (38), the following expressions for the kinetic energy and strain energy are obtained

$$T = \frac{1}{2}\iint_{\Omega} \sum_n \sum_{i_n} \sum_{j_n} \Lambda^{(n)i_n j_n} \dot{u}_i^{(n)i_n} \rho^{(n)} \dot{u}_i^{(n)j_n} \, dx_1 dx_2 \tag{44}$$

$$\begin{aligned} \Pi = \frac{1}{2}\iint_{\Omega} \sum_n \sum_{i_n} \sum_{j_n} \Lambda^{(n)i_n j_n} \Big(& \varepsilon_{ij}^{(n)i_n} C_{ijkl}^{(n)} \varepsilon_{kl}^{(n)j_n} \\ & - 2\varepsilon_{ij}^{(n)i_n} e_{kij}^{(n)} E_k^{(n)j_n} - E_i^{(n)i_n} \in_{ik}^{(n)} E_k^{(n)j_n} \Big) dx_1 dx_2 \end{aligned} \tag{45}$$

Analytical solution for layered piezoelectric rectangular plate

In this section, we study the free vibration of the layered piezoelectric rectangular plate with simply supported edges. The boundary conditions for the simply supported plate with electrically grounded edges are written as

$$\begin{aligned} & \sigma_{11}^{(n)} = u_2^{(n)} = u_3^{(n)} = \varphi^{(n)} = 0 \text{ at } x_1 = 0 \text{ and } x_1 = a \\ & \sigma_{22}^{(n)} = u_1^{(n)} = u_3^{(n)} = \varphi^{(n)} = 0 \text{ at } x_2 = 0 \text{ and } x_2 = b \end{aligned} \tag{46}$$

where a and b are the length and width of the plate.

To satisfy boundary conditions (46), we seek the analytical solution of the problem in the following form

$$\begin{aligned} u_1^{(n)i_n} &= u_{1rs}^{(n)i_n} e^{i\omega_{rs}t} \cos\frac{r\pi x_1}{a} \sin\frac{s\pi x_2}{b} \\ u_2^{(n)i_n} &= u_{2rs}^{(n)i_n} e^{i\omega_{rs}t} \sin\frac{r\pi x_1}{a} \cos\frac{s\pi x_2}{b} \\ u_3^{(n)i_n} &= u_{3rs}^{(n)i_n} e^{i\omega_{rs}t} \sin\frac{r\pi x_1}{a} \sin\frac{s\pi x_2}{b} \\ \varphi^{(n)i_n} &= \varphi_{rs}^{(n)i_n} e^{i\omega_{rs}t} \sin\frac{r\pi x_1}{a} \sin\frac{s\pi x_2}{b} \end{aligned} \tag{47}$$

where r and s are the half-wave numbers in x_1 and x_2 directions; $u_{irs}^{(n)i_n}$ and $\varphi_{rs}^{(n)i_n}$ are the amplitudes of the displacements and electric potentials of SaS; ω_{rs} is the frequency in radians per second; and $i = \sqrt{-1}$ is the imaginary unit.

Substituting equation (47) in equations (9), (16), (25), (30), (44), and (45) and using Hamilton's principle (33), we arrive at the homogeneous system of linear equations of order $4N_{\text{SaS}}$

$$\frac{\partial(T - \Pi)}{\partial \mathbf{W}_{rs}} = \mathbf{0}, \quad \frac{\partial(T - \Pi)}{\partial \mathbf{\Phi}_{rs}} = \mathbf{0} \tag{48}$$

where $\mathbf{W}_{rs}$ and $\mathbf{\Phi}_{rs}$ are the unknown column vectors of order $3N_{\text{SaS}}$ and N_{SaS} given by

$$\begin{aligned} \mathbf{W}_{rs} &= \left[\mathbf{W}_{1rs}^{\mathrm{T}} \; \mathbf{W}_{2rs}^{\mathrm{T}} \; \mathbf{W}_{3rs}^{\mathrm{T}} \right]^{\mathrm{T}} \\ \mathbf{W}_{irs} &= \Big[u_{irs}^{[0]} \; u_{irs}^{(1)2} \; \ldots \; u_{irs}^{(1)I_1-1} \; u_{irs}^{[1]} \; u_{irs}^{(2)2} \; \ldots \; u_{irs}^{(N-1)I_{N-1}-1} \\ & \qquad u_{irs}^{[N-1]} \; u_{irs}^{(N)2} \; \ldots \; u_{irs}^{(N)I_N-1} \; u_{irs}^{[N]} \Big]^{\mathrm{T}} \end{aligned} \tag{49}$$

$$\begin{aligned} \mathbf{\Phi}_{rs} = \Big[& \varphi_{rs}^{[0]} \; \varphi_{rs}^{(1)2} \; \ldots \; \varphi_{rs}^{(1)I_1-1} \; \varphi_{rs}^{[1]} \; \varphi_{rs}^{(2)2} \; \ldots \; \varphi_{rs}^{(N-1)I_{N-1}-1} \\ & \varphi_{rs}^{[N-1]} \; \varphi_{rs}^{(N)2} \; \ldots \; \varphi_{rs}^{(N)I_N-1} \; \varphi_{rs}^{[N]} \Big]^{\mathrm{T}} \end{aligned} \tag{50}$$

where $N_{\text{SaS}} = \sum_n I_n - N + 1$ is the total number of SaS.

The homogeneous system (48) can be expressed as (no summation is needed)

$$\left(\begin{bmatrix} \mathbf{K}_{rs}^{uu} & \mathbf{K}_{rs}^{u\varphi} \\ \mathbf{K}_{rs}^{\varphi u} & \mathbf{K}_{rs}^{\varphi\varphi} \end{bmatrix} - \omega_{rs}^2 \begin{bmatrix} \mathbf{M}_{rs} & \mathbf{0} \\ \mathbf{0} & \mathbf{0} \end{bmatrix} \right) \begin{bmatrix} \mathbf{W}_{rs} \\ \mathbf{\Phi}_{rs} \end{bmatrix} = \mathbf{0} \quad (51)$$

where $\mathbf{K}_{rs}^{uu}$, $\mathbf{K}_{rs}^{u\varphi}$, $\mathbf{K}_{rs}^{\varphi u} = (\mathbf{K}_{rs}^{u\varphi})^{\mathrm{T}}$, $\mathbf{K}_{rs}^{\varphi\varphi}$, and $\mathbf{M}_{rs}$ are the stiffness and inertial matrices. Eliminating $\mathbf{\Phi}_{rs}$ from the second row of (51), one finds

$$\mathbf{\Phi}_{rs} = -(\mathbf{K}_{rs}^{\varphi\varphi})^{-1}\mathbf{K}_{rs}^{\varphi u}\mathbf{W}_{rs} \quad (52)$$

Inserting then equation (52) in the second row of (51), the following reduced homogeneous system is obtained

$$(\mathbf{K}_{rs} - \omega_{rs}^2\mathbf{M}_{rs})\mathbf{W}_{rs} = \mathbf{0} \quad (53)$$

$$\mathbf{K}_{rs} = \mathbf{K}_{rs}^{uu} - \mathbf{K}_{rs}^{u\varphi}(\mathbf{K}_{rs}^{\varphi\varphi})^{-1}\mathbf{K}_{rs}^{\varphi u} \quad (54)$$

which has a non-trivial solution only if

$$\det\,(\mathbf{K}_{rs} - \omega_{rs}^2\mathbf{M}_{rs}) = 0 \quad (55)$$

where $\mathbf{K}_{rs}$ is the stiffness matrix of order $3N_{\mathrm{SaS}} \times 3N_{\mathrm{SaS}}$.

The polynomial equation (55) has to be solved to obtain the circular frequencies $0 < \omega_{rs}^{(1)} < \omega_{rs}^{(2)} < \cdots < \omega_{rs}^{(3N_{\mathrm{SaS}})}$ arranged in an increasing order. The eigenvectors $\mathbf{W}_{rs}^{(q)}$ associated with the corresponding eigenvalues $\lambda_{rs}^{(q)} = (\omega_{rs}^{(q)})^2$ can be evaluated using (53), where the superscript $q = 1, 2, \ldots, 3N_{\mathrm{SaS}}$ stands for the number of through-thickness modes.

The described algorithm was performed with the Symbolic Math Toolbox, which incorporates symbolic computations into the numeric environment of MATLAB. This makes it possible to obtain the analytical solutions for layered piezoelectric rectangular plates in the framework of the SaS formulation, which *asymptotically* approach the 3D exact solutions of electroelasticity as the number of SaS goes to infinity.

Numerical examples

Here, we study simply supported homogeneous and layered piezoelectric rectangular plates with different electric boundary conditions, namely, the open-circuit surface conditions [OC/OC]

$$\begin{aligned} &\sigma_{13}^{(1)} = \sigma_{23}^{(1)} = \sigma_{33}^{(1)} = D_3^{(1)} = 0 \ \text{ at } \ x_3 = -h/2 \\ &\sigma_{13}^{(N)} = \sigma_{23}^{(N)} = \sigma_{33}^{(N)} = D_3^{(N)} = 0 \ \text{ at } \ x_3 = h/2 \end{aligned} \quad (56)$$

the closed-circuit surface conditions [CC/CC]

$$\begin{aligned} &\sigma_{13}^{(1)} = \sigma_{23}^{(1)} = \sigma_{33}^{(1)} = \varphi^{(1)} = 0 \ \text{ at } \ x_3 = -h/2 \\ &\sigma_{13}^{(N)} = \sigma_{23}^{(N)} = \sigma_{33}^{(N)} = \varphi^{(N)} = 0 \ \text{ at } \ x_3 = h/2 \end{aligned} \quad (57)$$

and their combination on the bottom and top surfaces [OC/CC]

$$\begin{aligned} &\sigma_{13}^{(1)} = \sigma_{23}^{(1)} = \sigma_{33}^{(1)} = D_3^{(1)} = 0 \ \text{ at } \ x_3 = -h/2 \\ &\sigma_{13}^{(N)} = \sigma_{23}^{(N)} = \sigma_{33}^{(N)} = \varphi^{(N)} = 0 \ \text{ at } \ x_3 = h/2 \end{aligned} \quad (58)$$

Table 1. Material properties.

Material	PZT-4	Graphite-epoxy
E_1 (GPa)	81.3	172.5
E_2 (GPa)	81.3	6.9
E_3 (GPa)	64.5	6.9
G_{12} (GPa)	30.6	3.45
G_{13} (GPa)	25.6	3.45
G_{23} (GPa)	25.6	1.38
ν_{12}	0.329	0.25
ν_{13}	0.432	0.25
ν_{23}	0.432	0.35
e_{311} (C/m^2)	−5.2	0.0
e_{322} (C/m^2)	−5.2	0.0
e_{333} (C/m^2)	15.08	0.0
e_{113} (C/m^2)	12.72	0.0
e_{223} (C/m^2)	12.72	0.0
$\in_{11}/\in_0$	1475	3.5
$\in_{22}/\in_0$	1475	3.0
$\in_{33}/\in_0$	1300	3.0
ρ (kg/m^3)	7600	1800

Vacuum permittivity $\in_0 = 8.854$ pF/m.

Single-layer piezoelectric square plate

Consider first a piezoelectric square plate composed of PZT-4 polarized in the thickness direction. The material properties of the piezoceramic are given in Table 1. To compare the results derived with the results of Heyliger and Saravanos (1995), we accept $\rho = 1\,\mathrm{kg/m^3}$ and introduce the scaled frequencies $\bar{\omega}_{rs}^{(q)} = \omega_{rs}^{(q)}/100$. Additionally, we introduce the dimensionless variables at crucial points as functions of the thickness coordinate

$$\begin{aligned} \bar{u}_1 &= u_1(0,\, b/2s,\, z)a/hu_3^* \\ \bar{u}_3 &= u_3(a/2r,\, b/2s,\, z)/u_3^* \\ \bar{\sigma}_{11} &= \sigma_{11}(a/2r,\, b/2s,\, z)a^2/E_0hu_3^* \\ \bar{\sigma}_{22} &= \sigma_{22}(a/2r,\, b/2s,\, z)a^2/E_0hu_3^* \\ \bar{\sigma}_{12} &= \sigma_{12}(0,\, 0,\, z)a^2/E_0hu_3^* \\ \bar{\sigma}_{13} &= \sigma_{13}(0,\, b/2s,\, z)a^3/E_0h^2u_3^* \\ \bar{\sigma}_{23} &= \sigma_{23}(a/2r,\, 0,\, z)a^3/E_0h^2u_3^* \\ \bar{\sigma}_{33} &= \sigma_{33}(a/2r,\, b/2s,\, z)a^4/E_0h^3u_3^* \\ \bar{\varphi} &= 10\varphi(a/2r,\, b/2s,\, z)d_0a^2/h^2u_3^* \\ \bar{D}_3 &= D_3(a/2r,\, b/2s,\, z)a^4/d_0E_0h^3u_3^* \end{aligned} \quad (59)$$

where $z = x_3/h$ is the dimensionless thickness coordinate; $u_3^* = u_3(a/2r,\, b/2s,\, 0)$ is the maximum transverse displacement of the middle surface; $E_0 = 81.3 \times 10^9$ Pa and $d_0 = 289.1 \times 10^{-12}$ m/V are the representative moduli and $h = 0.01$ m.

Tables 2 to 5 list the results of the convergence study for boundary conditions (56) and (57) due to the increasing number of SaS located at Chebyshev polynomial nodes, that is, the bottom and top surfaces are

Table 2. Results of the convergence study for a single-layer piezoelectric square plate with [OC/OC] boundary conditions and $a/h = 4$.

I_1	$\bar{\omega}_{11}^{(1)}$	$\bar{\omega}_{11}^{(2)}$	$\bar{\omega}_{11}^{(3)}$	$\bar{\omega}_{11}^{(4)}$	$\bar{\omega}_{11}^{(5)}$	$\bar{\omega}_{11}^{(6)}$
3	99773.8143357434	194255.204684596	355705.725011536	587311.743920598	788991.859246281	1181597.51575243
5	98228.1245520025	194255.204684596	355100.122831571	539015.380716002	691503.966823278	964539.136021171
7	98227.9520520980	194255.204684596	355099.905033162	538884.982090899	690736.303521442	960124.399484351
9	98227.9520500420	194255.204684597	355099.905022542	538884.920204224	690735.148147172	960099.360992508
11	98227.9520500058	194255.204684595	355099.905022540	538884.920196270	690735.147691658	960099.320944723
13	98227.9520500840	194255.204684597	355099.905022543	538884.920196277	690735.147691594	960099.320920497
15	98227.9520500547	194255.204684605	355099.905022544	538884.920196273	690735.147691593	960099.320920488
17	98227.9520499611	194255.204684595	355099.905022538	538884.920196275	690735.147691596	960099.320920484
Messina	98227.9	194255.	355100.	538885.	690735.	960100.
Heyliger	98231.7	194255.	355110.	538885.	690767.	960103.

Table 3. Results of the convergence study for a single-layer piezoelectric square plate with [CC/CC] boundary conditions and $a/h = 4$.

I_1	$\bar{\omega}_{11}^{(1)}$	$\bar{\omega}_{11}^{(2)}$	$\bar{\omega}_{11}^{(3)}$	$\bar{\omega}_{11}^{(4)}$	$\bar{\omega}_{11}^{(5)}$	$\bar{\omega}_{11}^{(6)}$
3	98381.3101156504	194255.204684596	327998.435812103	587311.743920598	663373.310160145	1162099.61911516
5	96926.8955059357	194255.204684596	327663.080845491	539015.380716002	609435.616906090	963177.551134399
7	96926.7319888342	194255.204684598	327662.988261812	538884.982090899	609186.118325569	958942.424670762
9	96926.7320302374	194255.204684598	327662.988259752	538884.920204225	609185.912717077	958918.567357662
11	96926.7319879252	194255.204684594	327662.988259885	538884.920196268	609185.912669931	958918.529424406
13	96926.7319776672	194255.204684599	327662.988259936	538884.920196275	609185.912671180	958918.529391287
15	96926.7320665448	194255.204684608	327662.988259946	538884.920196277	609185.912674578	958918.529390630
17	96926.7320090039	194255.204684595	327662.988260058	538884.920196277	609185.912670717	958918.529392859
Messina	96926.7	194255.	327663.	538885.	609186.	958919.
Heyliger	96929.9	194255.	327663.	538885.	609186.	958922.

Table 4. Results of the convergence study for a single-layer piezoelectric square plate with [OC/OC] boundary conditions for $a/h = 4$ and $r = s = q = 1$.

I_1	$\bar{u}_1(0.5)$	$\bar{u}_3(0.5)$	$\bar{\sigma}_{11}(0.5)$	$\bar{\sigma}_{12}(0.5)$	$\bar{\sigma}_{13}(0)$	$\bar{\sigma}_{33}(0.25)$	$\bar{\varphi}(0.5)$	$\bar{D}_3(0.25)$
3	−1.21272382309	0.940769658154	7.22824351303	−2.86795715019	5.54290320725	0.34810561221	5.38044551434	−0.42130308345
5	−1.22652010011	0.946941768266	7.30587983695	−2.90058381307	7.07503884646	2.64662624240	5.16021052452	2.66860431240
7	−1.22650085906	0.946926526497	7.30541592344	−2.90053831012	7.05693301220	2.63701938630	5.16009752719	2.65332911732
9	−1.22650089267	0.946926552439	7.30541455502	−2.90053838959	7.05699743091	2.63700521091	5.16009766815	2.65331135257
11	−1.22650089263	0.946926552413	7.30541455184	−2.90053838952	7.05699731999	2.63700526102	5.16009766801	2.65331143516
13	−1.22650089263	0.946926552413	7.30541455184	−2.90053838952	7.05699732011	2.63700526101	5.16009766801	2.65331143513
15	−1.22650089263	0.946926552413	7.30541455184	−2.90053838951	7.05699732010	2.63700526101	5.16009766801	2.65331143512
17	−1.22650089263	0.946926552413	7.30541455183	−2.90053838951	7.05699732009	2.63700526095	5.16009766800	2.65331143511

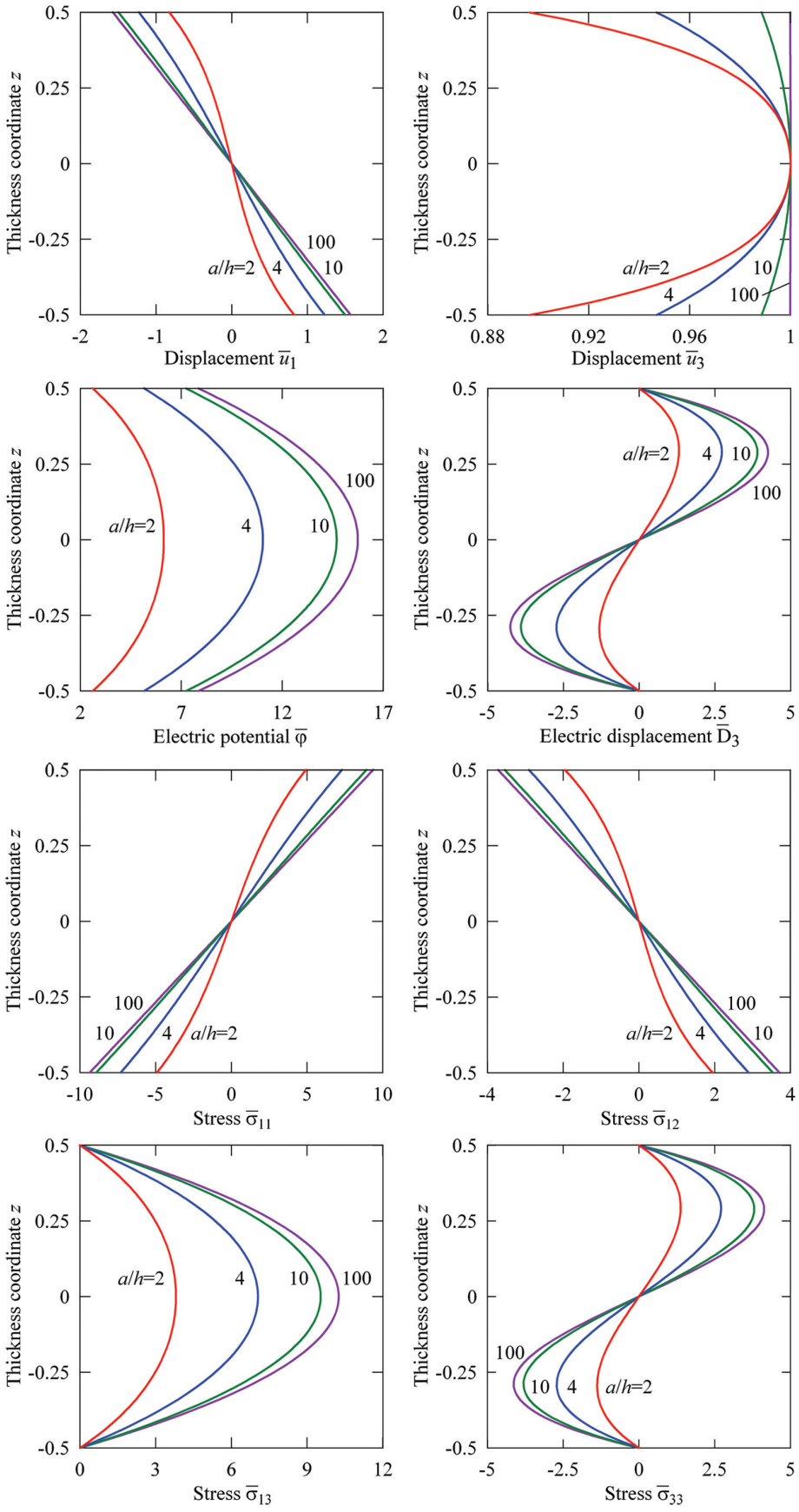

Figure 2. Through-thickness distributions of displacements, electric potential, electric displacement, and stresses for a single-layer piezoelectric square plate with [OC/OC] boundary conditions for $l_1 = 9$ and half-wave numbers $r = s = 1$ and $q = 1$.

Table 5. Results of the convergence study for a single-layer piezoelectric square plate with [CC/CC] boundary conditions for $a/h = 4$ and $r = s = q = 1$.

l_1	$\bar{u}_1(0.5)$	$\bar{u}_3(0.5)$	$\bar{\sigma}_{11}(0.5)$	$\bar{\sigma}_{12}(0.5)$	$\bar{\sigma}_{13}(0)$	$\bar{\sigma}_{33}(0.25)$	$\bar{\varphi}(0)$	$\bar{D}_3(0.25)$
3	−1.14529544630	0.946968905246	7.08611299681	−2.70849652805	5.42322466931	0.35979565794	6.68022113485	6.05290948360
5	−1.16130608839	0.952655762986	7.17054583018	−2.74635991837	6.90172154199	2.59240554545	6.53667293828	8.65812306704
7	−1.16128891589	0.952640936927	7.17011730656	−2.74631930731	6.88424367757	2.58309798066	6.53696260997	8.64337058079
9	−1.16128894667	0.952640962239	7.17011600170	−2.74631938010	6.88430586505	2.58308403650	6.53696229826	8.64335483205
11	−1.16128894666	0.952640962142	7.17011597765	−2.74631938006	6.88430575367	2.58308408543	6.53696227254	8.64335485884
13	−1.16128894667	0.952640962125	7.17011591754	−2.74631938007	6.88430575172	2.58308409063	6.53696226177	8.64335517613
15	−1.16128894665	0.952640962310	7.17011601139	−2.74631938004	6.88430576434	2.58308408875	6.53696232983	8.64335535852
17	−1.16128894661	0.952640962170	7.17011601538	−2.74631937996	6.88430575598	2.58308408107	6.53696228496	8.64335487682

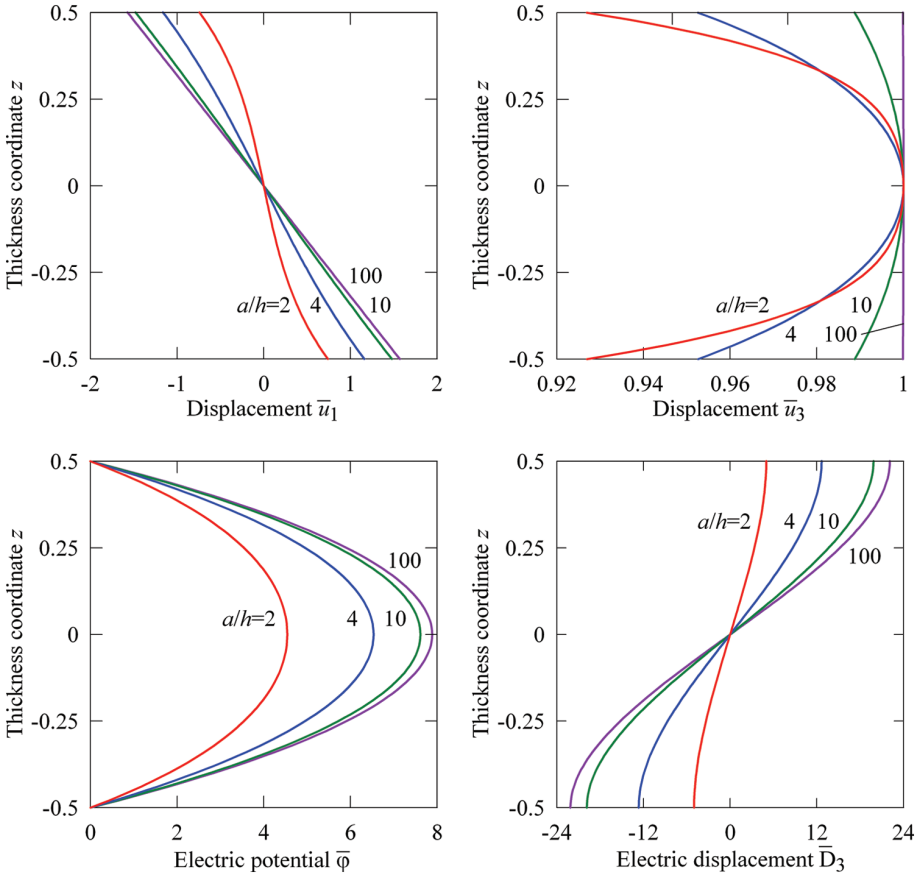

Figure 3. Through-thickness distributions of displacements, electric potential, and electric displacement for a single-layer piezoelectric square plate with [CC/CC] boundary conditions for $l_1 = 9$ and half-wave numbers $r = s = 1$ and $q = 1$.

Table 6. Natural frequencies $\bar{\omega}_{rs}^{(1)}$ of a single-layer piezoelectric square plate with different electric boundary conditions and half-wave numbers for $l_1 = 9$.

Frequency	$a/h = 2$	$a/h = 4$	$a/h = 10$	$a/h = 100$
$\bar{\omega}_{11}^{(1)}$, [OC/OC]	293801.	98228.0	18077.2	186.911
$\bar{\omega}_{11}^{(1)}$, [CC/CC]	288227.	96926.7	18012.9	186.903
$\bar{\omega}_{12}^{(1)}$, [OC/OC]	543827.	207264.	43183.7	467.019
$\bar{\omega}_{12}^{(1)}$, [CC/CC]	534352.	203517.	42859.9	466.972
$\bar{\omega}_{22}^{(1)}$, [OC/OC]	724558.	293801.	66347.3	746.851
$\bar{\omega}_{22}^{(1)}$, [CC/CC]	713023.	288227.	65662.3	746.731

not included into a set of SaS. This is important because using only Chebyshev polynomial nodes makes it possible to minimize uniformly the error due to the Lagrange interpolation. A comparison with the 3D analytical solutions (Heyliger and Saravanos, 1995; Messina and Carrera, 2015) is presented. As it turned out, the proposed SaS formulation provides from 12 to 14 right digits for the first six natural frequencies corresponding to half-wave numbers $r = s = 1$ (see, e.g. Table 2) utilizing 17 SaS inside the plate body. However, the increase of SaS to 19 gives a bit worse results and the choice of a more number of SaS lead to

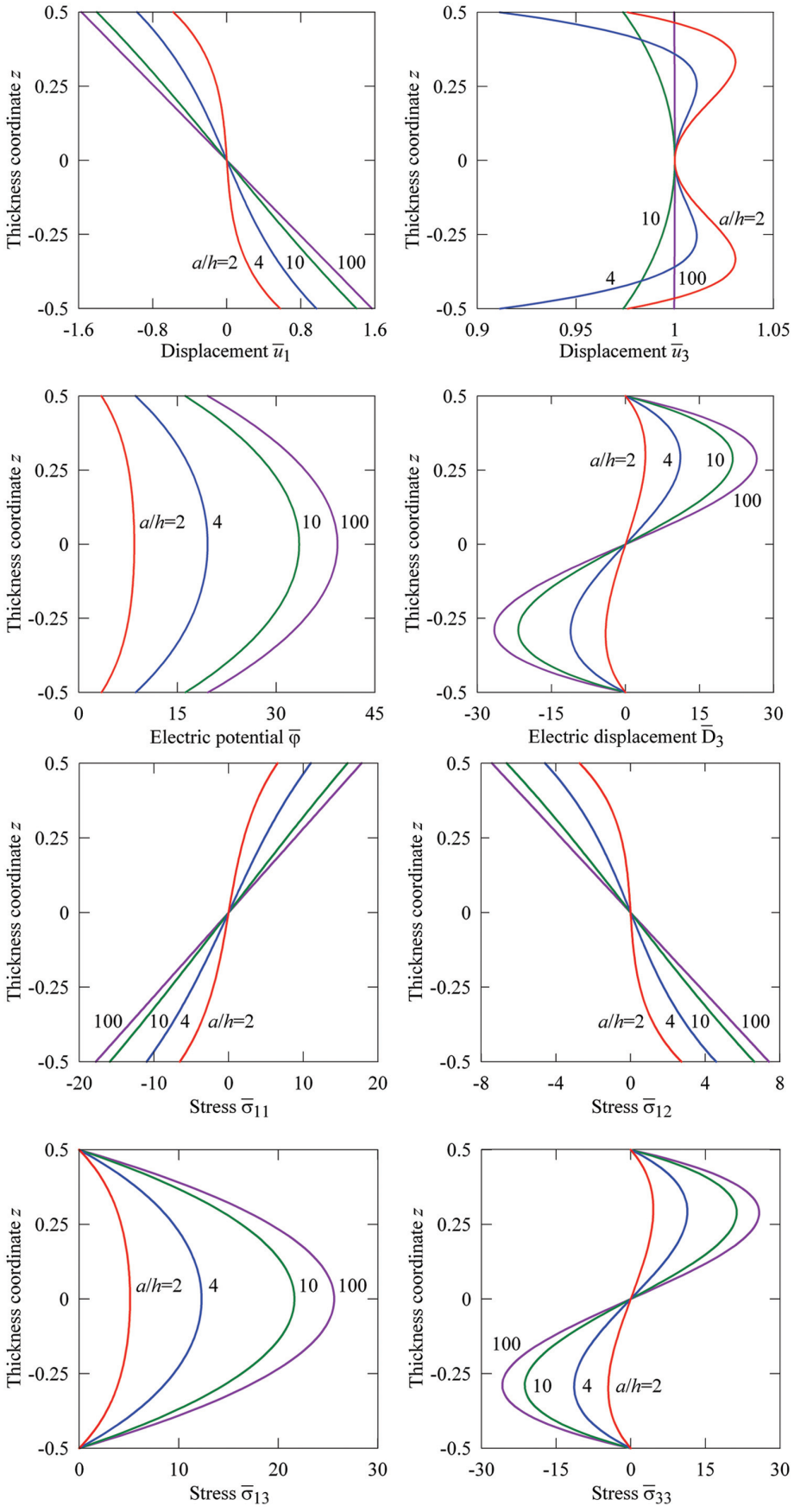

Figure 4. Through-thickness distributions of displacements, electric potential, electric displacement, and stresses for a single-layer piezoelectric square plate with [OC/OC] boundary conditions for $l_1 = 9$ and half-wave numbers $r = 1$, $s = 2$ and $q = 1$.

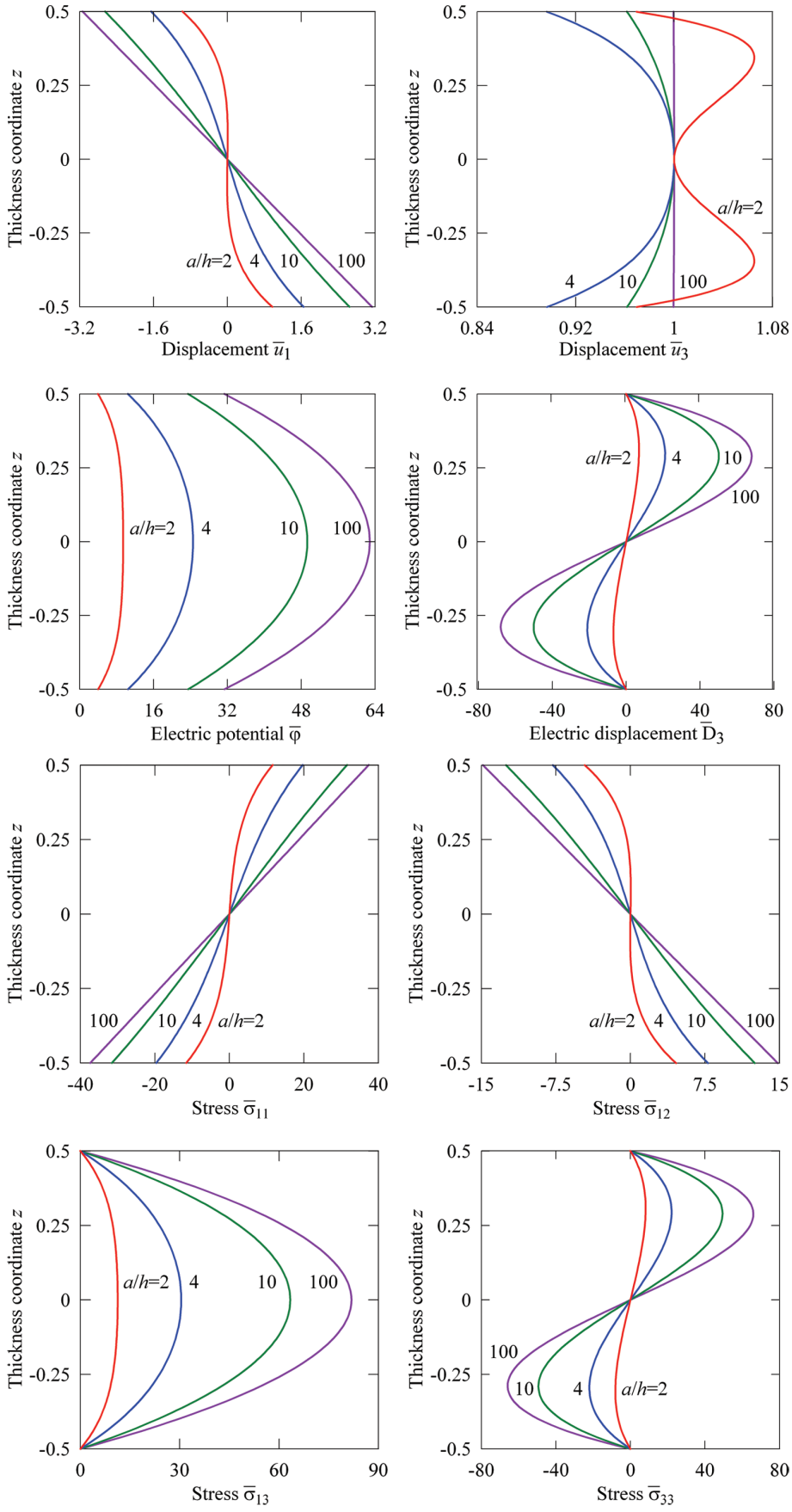

Figure 5. Through-thickness distributions of displacements, electric potential, electric displacement, and stresses for a single-layer piezoelectric square plate with [OC/OC] boundary conditions for $l_1 = 9$ and half-wave numbers $r = s = 2$ and $q = 1$.

Table 7. Results of the convergence study for a hybrid four-layer square plate with [OC/OC] boundary conditions and $a/h = 4$.

I_n	$\bar{\omega}_{11}^{(1)}$	$\bar{\omega}_{11}^{(2)}$	$\bar{\omega}_{11}^{(3)}$	$\bar{\omega}_{11}^{(4)}$	$\bar{\omega}_{11}^{(5)}$	$\bar{\omega}_{11}^{(6)}$
3	3.66263720355491	13.7798630431600	15.3568827772785	18.6690676457869	22.4805173192812	23.5567170949674
5	3.66169039500578	13.7791689442191	15.3523391788586	18.6678985666693	22.4792794125583	23.5509856633015
7	3.66169037401532	13.7791689147964	15.3523389097921	18.6678985480642	22.4792793724763	23.5509853105412
9	3.66169037415034	13.7791689147945	15.3523389097881	18.6678985480999	22.4792793724791	23.5509853105395

Table 8. Results of the convergence study for a hybrid four-layer square plate with [OC/CC] boundary conditions and $a/h = 4$.

I_n	$\bar{\omega}_{11}^{(1)}$	$\bar{\omega}_{11}^{(2)}$	$\bar{\omega}_{11}^{(3)}$	$\bar{\omega}_{11}^{(4)}$	$\bar{\omega}_{11}^{(5)}$	$\bar{\omega}_{11}^{(6)}$
3	3.65938664457603	13.7797203996059	15.3568794705302	18.6681893520410	22.4459180580976	23.5031266932395
5	3.65844537088379	13.7790263574561	15.3523360017163	18.6670216390431	22.4446656157571	23.4975079666010
7	3.65844534978032	13.7790263280384	15.3523357326587	18.6670216204038	22.4446655754685	23.4975076244451
9	3.65844534977213	13.7790263280356	15.3523357326530	18.6670216204152	22.4446655754657	23.4975076244402

Table 9. Results of the convergence study for a hybrid four-layer square plate with [CC/CC] boundary conditions and $a/h = 4$.

I_n	$\bar{\omega}_{11}^{(1)}$	$\bar{\omega}_{11}^{(2)}$	$\bar{\omega}_{11}^{(3)}$	$\bar{\omega}_{11}^{(4)}$	$\bar{\omega}_{11}^{(5)}$	$\bar{\omega}_{11}^{(6)}$
3	3.65618520016599	13.7795800290872	15.3568761100173	18.6672977302561	22.4140765604835	23.4472505782067
5	3.65524937852241	13.7788860428256	15.3523327729134	18.6661314012146	22.4128191567059	23.4417314749381
7	3.65524935727075	13.7788860134146	15.3523325038642	18.6661313825559	22.4128191167186	23.4417311425044
9	3.65524935730906	13.7788860134109	15.3523325038600	18.6661313825603	22.4128191167191	23.4417311425004

the divergence of the symbolic computation algorithm developed.

Figures 2 to 5 display the distributions of displacements, electric potential, electric displacement, and stresses through the thickness for different values of the slenderness ratio a/h and different half-wave numbers taking 9 SaS located at Chebyshev polynomial nodes. These results demonstrate convincingly the high potential of the developed piezoelectric plate formulation because the boundary conditions on bottom and top surfaces for the transverse components of the stress tensor and electric displacement vector are satisfied with a high accuracy. Table 6 lists the natural frequencies of the piezoceramic plate with different electric boundary conditions, slenderness ratios, and half-wave numbers. It is seen that the use of closed-circuit surface conditions leads to slightly less frequencies for all values of the slenderness ratio and half-wave numbers considered.

Hybrid four-layer square plate

Consider next a simply supported two-ply square plate [0/90] made of the graphite epoxy composite and covered with PZT-4 piezoelectric layers at the bottom and at the top. Therefore, we deal here with a hybrid four-layer plate [PZT/0/90/PZT] with ply thicknesses [0.25h/0.25h/0.25h/0.25h]. The material properties of the graphite epoxy and PZT-4 are given in Table 1. To evaluate the results effectively, we utilize the dimensionless variables at crucial points (59) except for the dimensionless frequency and electric displacement, which are defined as

$$\begin{aligned} \bar{\omega}_{rs}^{(q)} &= \omega_{rs}^{(q)} a^2 \sqrt{\rho_0/E_0}/h \\ \bar{D}_3 &= 100 D_3(a/2r,\, b/2s,\, z) a^2/d_0 E_0 h u_3^* \end{aligned} \tag{60}$$

where $E_0 = 81.3 \times 10^9\,\text{Pa}$, $d_0 = 289.1 \times 10^{-12}\,\text{m/V}$, and $\rho_0 = 7600\,\text{kg/m}^3$ are the representative moduli and $a = b = 1\,\text{m}$.

The data listed in Tables 7 to 9 show that the SaS formulation allows the reproducing of the 3D exact solution for layered piezoelectric plates with a high accuracy by choosing a sufficiently large number of SaS throughout the plate. Here, the bottom and top surfaces and interfaces as well are included into a set of SaS. Nevertheless, the accuracy of calculations is not worse than for a single-layer plate considered in a previous section, where all SaS are located at Chebyshev polynomial nodes. It is seen that the use of 25 SaS corresponding to the choice of 7 SaS inside each layer provides from 10 to 13 right digits for the first six natural frequencies. However, to achieve the high accuracy for electric displacements and stresses, which are evaluated through the constitutive equations (39) and (40), the more SaS should be taken. As can be seen from Tables 10 to 12, the use of 29 SaS that corresponds to

Table 10. Results of the convergence study for a hybrid four-layer square plate with [OC/OC] boundary conditions for $a/h = 4$ and $r = s = q = 1$.

I_n	$\bar{u}_1(0.5)$	$\bar{u}_3(0.5)$	$\bar{\sigma}_{11}(0.5)$	$\bar{\sigma}_{12}(0.5)$	$\bar{\sigma}_{13}(0.125)$	$\bar{\sigma}_{33}(0.125)$	$\bar{\varphi}(0.375)$	$\bar{D}_3(0.375)$
3	−0.498237625833	0.998174116456	3.43635511813	−1.47219110995	1.33892650654	0.751414619911	2.40312403176	1.62054949671
4	−0.498251611468	0.998164366994	3.42112506431	−1.47246106059	1.33741742156	0.727624775548	2.40136391579	1.94665640332
5	−0.498253485647	0.998164207746	3.41459167869	−1.47246007640	1.33742284722	0.727679678142	2.40107352220	1.94559398969
6	−0.498253484586	0.998164206549	3.41457035152	−1.47246009747	1.33741821666	0.727916197233	2.40107366758	1.94518131736
7	−0.498253484646	0.998164206541	3.41456633481	−1.47246009743	1.33741820208	0.727915997622	2.40107372174	1.94518155823
8	−0.498253484653	0.998164206542	3.41456632778	−1.47246009743	1.33741823074	0.727915051140	2.40107372173	1.94518169069
9	−0.498253484643	0.998164206538	3.41456632687	−1.47246009742	1.33741823074	0.727915051108	2.40107372173	1.94518169050

Table 11. Results of the convergence study for a hybrid four-layer square plate with [OC/CC] boundary conditions for $a/h = 4$ and $r = s = q = 1$.

I_n	$\bar{u}_1(0.5)$	$\bar{u}_3(0.5)$	$\bar{\sigma}_{11}(0.5)$	$\bar{\sigma}_{12}(0.5)$	$\bar{\sigma}_{13}(0.125)$	$\bar{\sigma}_{33}(0.125)$	$\bar{\varphi}(0.375)$	$\bar{D}_3(0.375)$
3	−0.490733279032	0.998522684257	3.42500207286	−1.45263494602	1.33623641184	0.755744094938	1.11611611194	7.31149102272
4	−0.490754291497	0.998512436239	3.40996185838	−1.45292519159	1.33475792264	0.732275199825	1.11568384263	7.61047859609
5	−0.490756182924	0.998512276163	3.40351961785	−1.45292430014	1.33476340895	0.732329373165	1.11539502969	7.60940313060
6	−0.490756181648	0.998512274971	3.40349847948	−1.45292432085	1.33475871361	0.732562984746	1.11539514334	7.60900235263
7	−0.490756181705	0.998512274964	3.40349451345	−1.45292432081	1.33475869895	0.732562787543	1.11539519807	7.60900259125
8	−0.490756181718	0.998512274966	3.40349450650	−1.45292432081	1.33475872780	0.732561852627	1.11539519807	7.60900272110
9	−0.490756181711	0.998512274965	3.40349450562	−1.45292432081	1.33475872782	0.732561852804	1.11539519806	7.60900272120

Table 12. Results of the convergence study for a hybrid four-layer square plate with [CC/CC] boundary conditions for $a/h = 4$ and $r = s = q = 1$.

I_n	$\bar{u}_1(0.5)$	$\bar{u}_3(0.5)$	$\bar{\sigma}_{11}(0.5)$	$\bar{\sigma}_{12}(0.5)$	$\bar{\sigma}_{13}(0.125)$	$\bar{\sigma}_{33}(0.125)$	$\bar{\varphi}(0.375)$	$\bar{D}_3(0.375)$
3	−0.490733385092	0.998471761705	3.42443224330	−1.45245587891	1.33564614141	0.750087198051	1.11539837249	7.21926971532
4	−0.490754582456	0.998461595190	3.40940038880	−1.45274706781	1.33417647756	0.726505736014	1.11496759221	7.51855109141
5	−0.490756469992	0.998461435927	3.40295745575	−1.45274616511	1.33418194533	0.726560243217	1.11467875539	7.51747608842
6	−0.490756468735	0.998461434727	3.40293632295	−1.45274618588	1.33417722689	0.726794965829	1.11467886913	7.51707527026
7	−0.490756468797	0.998461434721	3.40293235594	−1.45274618584	1.33417721219	0.726794767774	1.11467892387	7.51707550878
8	−0.490756468795	0.998461434719	3.40293234894	−1.45274618584	1.33417724109	0.726793828024	1.11467892386	7.51707563867
9	−0.490756468807	0.998461434724	3.40293234813	−1.45274618585	1.33417724114	0.726793828960	1.11467892386	7.51707563879

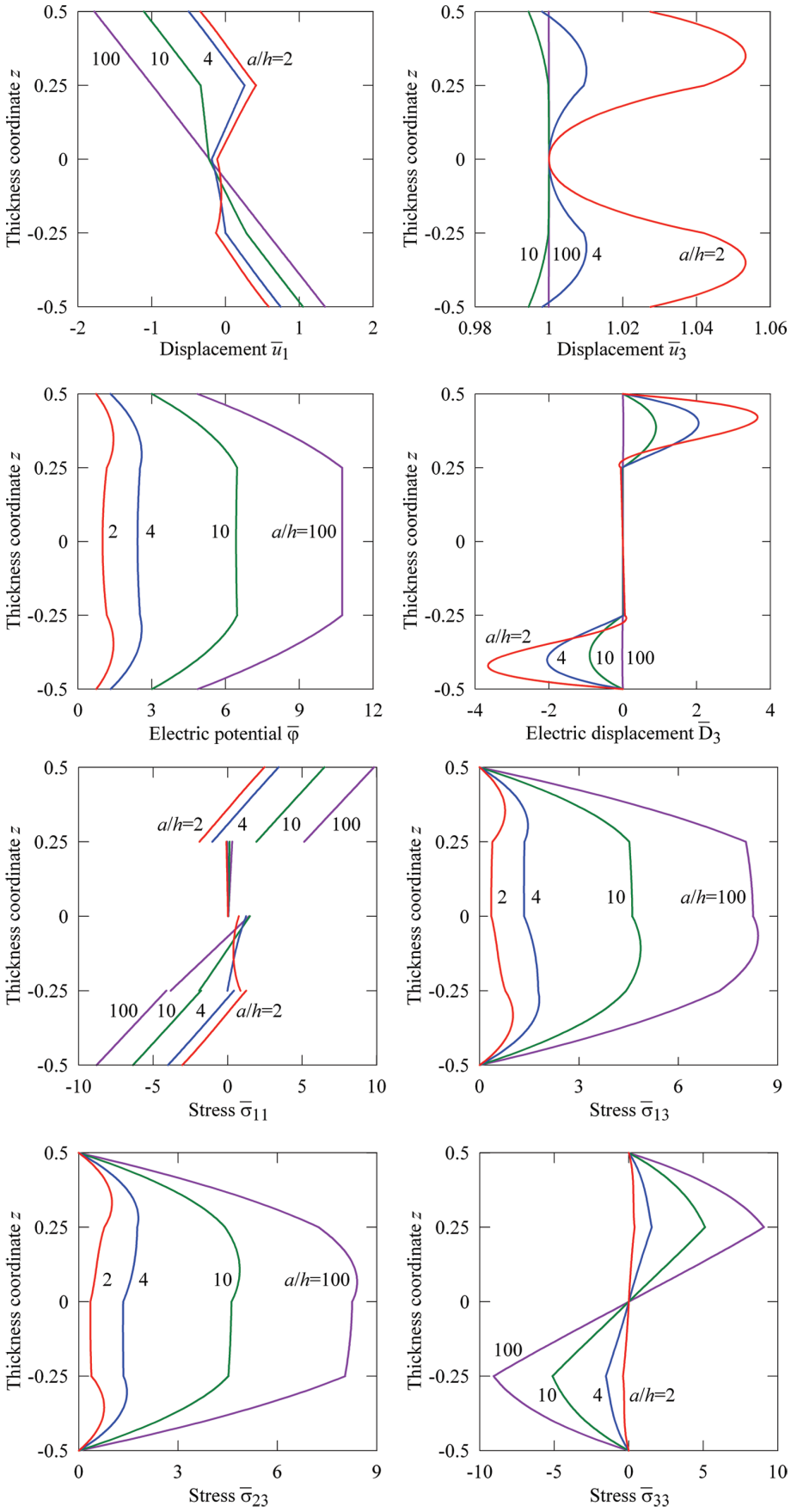

Figure 6. Through-thickness distributions of displacements, electric potential, electric displacement, and stresses for a hybrid four-layer square plate with [OC/OC] boundary conditions for $l_1 = l_2 = l_3 = l_4 = 7$ and half-wave numbers $r = s = 1$ and $q = 1$.

Table 13. Fundamental frequency $\bar{\omega}_{11}^{(1)}$ of a hybrid four-layer square plate with different electric boundary conditions and slenderness ratios for $l_1 = l_2 = l_3 = l_4 = 7$.

Boundary conditions	$a/h = 2$	$a/h = 4$	$a/h = 10$	$a/h = 100$
[OC/OC]	2.33432382	3.66169037	6.09657272	7.93449125
[OC/CC]	2.32897463	3.65844535	6.09481234	7.93443119
[CC/CC]	2.32363758	3.65524936	6.09322509	7.93442753

the choice of 8 SaS inside each layer provides from 9 to 12 right digits for these variables at crucial points.

Figure 6 presents the through-thickness distributions of displacements, electric potential, electric displacement, and stresses in the case of [OC/OC] electric boundary conditions for different slenderness ratios by choosing seven SaS inside each layer. It is seen that the boundary conditions on bottom and top surfaces and the continuity conditions at interfaces for transverse stress and electric displacement components are satisfied correctly. Figures 7 and 8 show only distributions of the electric potential and electric displacement through the thickness of the plate for [OC/CC] and [CC/CC] boundary conditions because the through-thickness distributions of displacements and stresses are very similar to those depicted in Figure 6 and, therefore, they are not displayed here. Table 13 lists additionally the fundamental frequencies of the hybrid four-layer plate with different electric boundary conditions and various slenderness ratios. It is seen that the use of the closed-circuit surface condition yields again slightly less frequencies for all values of the slenderness ratio.

Conclusion

An efficient SaS formulation for the 3D free vibration analysis of layered piezoelectric plates has been proposed. It is based on a new concept of SaS located at

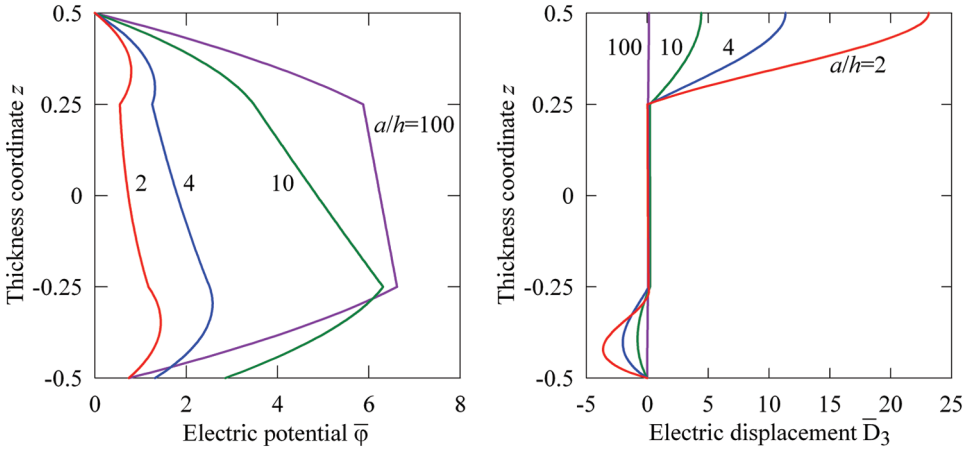

Figure 7. Through-thickness distributions of electric potential and electric displacement for a hybrid four-layer square plate with [OC/CC] boundary conditions for $l_1 = l_2 = l_3 = l_4 = 7$ and half-wave numbers $r = s = 1$ and $q = 1$.

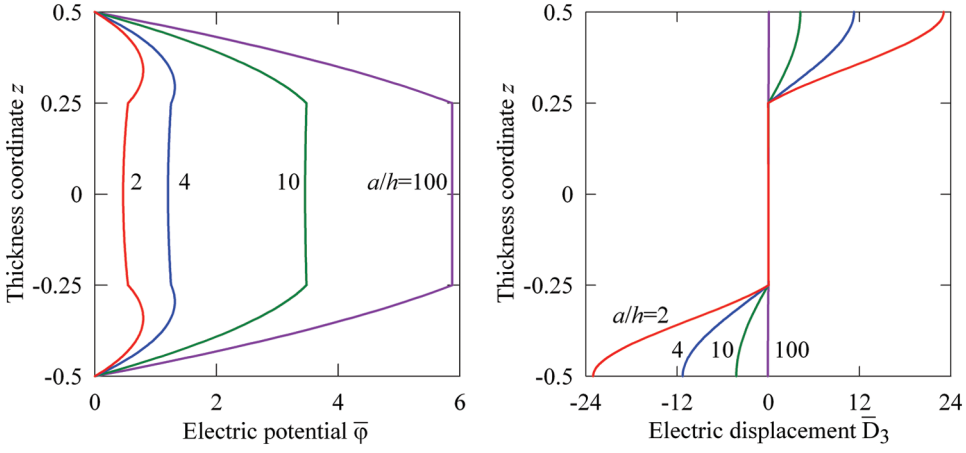

Figure 8. Through-thickness distributions of electric potential and electric displacement for a hybrid four-layer square plate with [CC/CC] boundary conditions for $l_1 = l_2 = l_3 = l_4 = 7$ and half-wave numbers $r = s = 1$ and $q = 1$.

Chebyshev polynomial nodes throughout the layers and interfaces as well. The use of only Chebyshev polynomial nodes makes it possible to minimize uniformly the error due to the Lagrange interpolation. Therefore, the developed SaS formulation gives an opportunity to obtain the analytical solutions for the free vibration of piezoelectric plates with a prescribed accuracy, which asymptotically approach the exact solutions of electroelasticity as the number of SaS goes to infinity.

Declaration of conflicting interests

The author(s) declared no potential conflicts of interest with respect to the research, authorship, and/or publication of this article.

Funding

The author(s) disclosed receipt of the following financial support for the research, authorship, and/or publication of this article: This work was supported by the Russian Science Foundation (Grant No. 15-19-30002) and the Russian Ministry of Education and Science (Grant No. 9.4914.2017).

References

Baillargeon BP and Vel SS (2005) Exact solution for the vibration and active damping of composite plates with piezoelectric shear actuators. *Journal of Sound and Vibration* 282: 781–804.

Brogan WL (1985) *Modern Control Theory*. Upper Saddle River, NJ: Prentice Hall.

Burden RL and Faires JD (2010) *Numerical Analysis*. 9th ed. Boston, MA: Brooks/Cole, Cengage Learning.

Carrera E (2002) Theories and finite elements for multilayered, anisotropic, composite plates and shells. *Archives of Computational Methods in Engineering* 9: 1–60.

Carrera E (2003) Theories and finite elements for multilayered plates and shells: a unified compact formulation with numerical assessment and benchmarking. *Archives of Computational Methods in Engineering* 10: 215–296.

Carrera E, Brischetto S and Cinefra M (2010) Variable kinematics and variational statements for free vibrations analysis of piezoelectric plates and shells. *Computer Modeling in Engineering & Sciences* 65(3): 259–341.

Carrera E, Brischetto S and Nali P (2011) *Plates and Shells for Smart Structures: Classical and Advanced Theories for Modeling and Analysis*. London: John Wiley & Sons.

Chen J, Chen H, Pan E, et al. (2007a) Modal analysis of magneto-electro-elastic plates using the state-vector approach. *Journal of Sound and Vibration* 304: 722–734.

Chen J, Pan E and Chen H (2007b) Wave propagation in magneto-electro-elastic multilayered plates. *International Journal of Solids and Structures* 44: 1073–1085.

Chen WQ and Ding HJ (2002) On free vibration of a functionally graded piezoelectric rectangular plate. *Acta Mechanica* 153: 207–216.

Chen WQ, Lee KY and Ding HJ (2005) On free vibration of non-homogeneous transversely isotropic magneto-electro-elastic plates. *Journal of Sound and Vibration* 279: 237–251.

Chen WQ, Xu RQ and Ding HJ (1998) On free vibration of a piezoelectric composite rectangular plate. *Journal of Sound and Vibration* 218: 741–748.

Cheng ZQ and Batra RC (2000) Three-dimensional asymptotic analysis of multiple-electroded piezoelectric laminates. *AIAA Journal* 38: 317–324.

Cheng ZQ, Lim CW and Kitipornchai S (2000) Three-dimensional asymptotic approach to inhomogeneous and laminated piezoelectric plates. *International Journal of Solids and Structures* 37: 3153–3175.

Deü JF and Benjeddou A (2005) Free-vibration analysis of laminated plates with embedded shear-mode piezoceramic layers. *International Journal of Solids and Structures* 42: 2059–2088.

Ding HJ, Xu RQ, Chi YW, et al. (1999) Free axisymmetric vibration of transversely isotropic piezoelectric circular plates. *International Journal of Solids and Structures* 36: 4629–4652.

D'Ottavio M, Ballhause D, Kröplin B, et al. (2006) Closed-form solutions for the free-vibration problem of multilayered piezoelectric shells. *Computers and Structures* 84: 1506–1518.

Frobenius G (1873) Ueber die Integration der linearen Differentialgleichungen durch Reihen. *Journal für die reine und angewandte Mathematik* 76: 214–235.

Gao JX, Shen YP and Wang J (1998) Three dimensional analysis for free vibration of rectangular composite laminates with piezoelectric layers. *Journal of Sound and Vibration* 213: 383–390.

Gol'denveizer AN (1961) *Theory of Thin Elastic Shells*. New York: Pergamon Press.

Heyliger P and Brooks S (1995) Free vibration of piezoelectric laminates in cylindrical bending. *International Journal of Solids and Structures* 32: 2945–2960.

Heyliger P and Saravanos DA (1995) Exact free-vibration analysis of laminated plates with embedded piezoelectric layers. *Journal of the Acoustical Society of America* 98: 1547–1557.

Kalamkarov AL and Kolpakov AG (2001) A new asymptotic model for a composite piezoelastic plate. *International Journal of Solids and Structures* 38: 6027–6044.

Kulikov GM (2001) Refined global approximation theory of multilayered plates and shells. *Journal of Engineering Mechanics* 127: 119–125.

Kulikov GM and Carrera E (2008) Finite deformation higher-order shell models and rigid-body motions. *International Journal of Solids and Structures* 45: 3153–3172.

Kulikov GM and Plotnikova SV (2011) On the use of a new concept of sampling surfaces in a shell theory. *Advanced Structured Materials* 15: 715–726.

Kulikov GM and Plotnikova SV (2013a) Three-dimensional exact analysis of piezoelectric laminated plates via a sampling surfaces method. *International Journal of Solids and Structures* 50: 1916–1929.

Kulikov GM and Plotnikova SV (2013b) A sampling surfaces method and its application to three-dimensional exact solutions for piezoelectric laminated shells. *International Journal of Solids and Structures* 50: 1930–1943.

Kulikov GM and Plotnikova SV (2013c) A new approach to three-dimensional exact solutions for functionally graded piezoelectric laminated plates. *Composite Structures* 106: 33–46.

Kulikov GM and Plotnikova SV (2014) Exact electroelastic analysis of functionally graded piezoelectric shells. *International Journal of Solids and Structures* 51: 13–25.

Kulikov GM and Plotnikova SV (2015) Exact 3D thermoelectroelastic analysis of piezoelectric plates through a sampling surfaces method. *Mechanics of Advanced Materials and Structures* 22: 33–43.

Kulikov GM and Plotnikova SV (2016) A hybrid-mixed four-node quadrilateral plate element based on sampling surfaces method for 3D stress analysis. *International Journal for Numerical Methods in Engineering* 108: 26–54.

Kulikov GM and Plotnikova SV (2017) An analytical approach to three-dimensional coupled thermoelectroelastic analysis of functionally graded piezoelectric plates. *Journal of Intelligent Material Systems and Structures* 28: 435–450.

Kulikov GM, Mamontov AA and Plotnikova SV (2015) Coupled thermoelectroelastic stress analysis of piezoelectric shells. *Composite Structures* 124: 65–76.

Kulikov GM, Plotnikova SV, Kulikov MG, et al. (2016) Three-dimensional vibration analysis of layered and functionally graded plates through sampling surfaces formulation. *Composite Structures* 152: 349–361.

Messina A and Carrera E (2015) Three-dimensional free vibration of multi-layered piezoelectric plates through approximate and exact analyses. *Journal of Intelligent Material Systems and Structures* 26: 489–504.

Ootao Y and Tanigawa Y (2000) Three-dimensional transient piezothermoelasticity for a rectangular composite plate composed of cross-ply and piezoelectric laminae. *International Journal of Engineering Science* 38: 47–71.

Ootao Y and Tanigawa Y (2005) Transient analysis of multilayered magneto-electro-thermoelastic strip due to nonuniform heat supply. *Composite Structures* 68: 471–480.

Pagano NJ (1970) Exact solutions for rectangular bidirectional composites and sandwich plates. *Journal of Composite Materials* 4: 20–34.

Pan E and Heyliger PR (2002) Free vibrations of simply supported and multilayered magneto-electro-elastic plates. *Journal of Sound and Vibration* 252: 429–442.

Reddy JN and Cheng (2001) Three-dimensional solutions of smart functionally graded plates. *Journal of Applied Mechanics* 68: 234–241.

Tiersten HF (1969) *Linear Piezoelectric Plate Vibrations*. New York: Plenum Publishers.

Tsai YH and Wu CP (2008) Dynamic responses of functionally graded magneto-electro-elastic shells with open-circuit surface conditions. *International Journal of Engineering Science* 46: 843–857.

Vel SS, Mewer RC and Batra RC (2004) Analytical solution for the cylindrical bending vibration of piezoelectric composite plates. *International Journal of Solids and Structures* 41: 1625–1643.

Vetyukov Y, Kuzin A and Krommer M (2011) Asymptotic splitting in the three-dimensional problem of elasticity for non-homogeneous piezoelectric plates. *International Journal of Solids and Structures* 48: 12–23.

Wu CP and Liu YC (2016) A review of semi-analytical numerical methods for laminated composite and multilayered functionally graded elastic/piezoelectric plates and shells. *Composite Structures* 147: 1–15.

Wu CP, Chiu KH and Wang YM (2008) A review on the three-dimensional analytical approaches of multilayered and functionally graded piezoelectric plates and shells. *Computers, Materials & Continua* 8: 93–132.

Zhong Z and Yu T (2006) Vibration of a simply supported functionally graded piezoelectric rectangular plate. *Smart Materials and Structures* 15: 1404–1412.